Reports

Thermodynamic Equilibrium and the Inorganic Origin of Organic Compounds

Abstract. *Theoretical and experimental support is presented for the hypothesis that many organic compounds may form under conditions of thermodynamic equilibrium. This possibility must be considered along with special effects of selective catalysts, radiation, and degradation from biological matter, in explaining the origin of organic compounds in carbonaceous chondrites. Similar considerations may apply to solar nebulas and planetary atmospheres. The equilibrium distribution of organic compounds at temperatures between 300°K and 1000°K and pressures of 10^{-6} to 50 atm for the C—H—O system have been computed. At moderate temperatures and low pressures, conditions where graphite production is inhibited, aromatic compounds may form even in the presence of large excesses of hydrogen. Such conditions exist in the solar nebula and in the atmospheres of some of the major planets. Equilibrium concentrations of a large number of compounds at 1000°K with nitrogen, sulfur, and chlorine added to the system have also been determined. In some cases, a limited equilibrium method is employed in which those few compounds which form with the most difficulty are excluded from the computations, while representatives of all other families of compounds are included. This approach is shown to be useful in the interpretation of certain experimental data in which complete equilibrium has not been attained. We have also found that gases, activated to the plasma state by a high-energy radio frequency field, recombine on cooling to yield product mixtures which are in qualitative agreement with those predicted by the equilibrium computations. We believe that such products can be profitably studied* as if *at a metastable limited equilibrium.*

In studies of the origin of organic mixtures such as asphalt, petroleum or the organic substances found in carbonaceous meteorites (*1*, *2*), it is important to account for the relative amounts of the various compounds present. Studier, Hayatsu and Anders (*1*), who have analyzed a number of carbonaceous chondrites by mass spectrometry, have proposed that the organic compounds they identified may have been formed under equilibrium or near equilibrium conditions in a solar nebula. They hold that neither biological processes nor high-energy radiation (without the influence of thermodynamic equilibration) could account for their observed proportions of compounds, particularly the preponderance of aromatic hydrocarbons and the high methane-to-ethane ratio. Their data did agree rather well, however, with a typical distribution calculated by Dayhoff, Lippincott, and Eck (*3*) for conditions of thermodynamic equilibrium for a C—H—O—N ideal gas system. Urey and Lewis (*4*), on the other hand, object to the hypothesis of an equilibrium origin of such compounds in the absence of graphite and maintain that the organic compounds detected by Studier *et al.* and other investigators in meteorites, could have been produced only by high-energy radiation or, in some instances, by living organisms. In a subsequent communication Studier, Hayatsu, and Anders (*5*) reported support for the equilibrium theory by the identification of products formed experimentally from carbon monoxide and hydrogen with heat alone, or with meteoritic material or inorganic compounds as catalysts.

The interest in this topic has led us to extend the scope of our computations in three ways: to include a larger number of elements and compounds, to widen the range of temperatures and pressures considered, and to take into account metastable conditions or limited thermodynamic equilibrium in which there is insufficient time for full equilibrium to be attained. These more general computations have led to some interesting new concepts concerning the application of equilibrium to planetary atmospheres and solar nebulas.

In our previous report (*3*) we presented the calculated distribution of elements among more than 100 compounds at 1 atm pressure and 500°K. At some C—H—O elemental proportions the formation of graphite was excluded because of the high activation energy of all reactions forming it. The present report describes calculations of thermodynamic equilibria in C—H—O systems at temperatures from 300° to 1000°K and pressures from 10^{-6} to 50 atm. Additional calculations including the elements N, S, and Cl at 1000°K are reported. Preliminary experiments on equilibria produced in a plasma discharge system are also presented.

The distribution of molecular species at chemical equilibrium is independent of the specific reactions by which that equilibrium is reached. There need be only one reversible reaction pathway from the major constituents that will produce each compound. At thermodynamic equilibrium, the equilibrium constants for all possible reactions among the constituents are simultaneously satisfied. The compound concentrations in an ideal gas mixture at equilibrium then depend only on the pressure, temperature, and elemental composition of the system, on the compounds assumed to be present in the system, and on the standard free energy of formation and molecular formula of each such compound.

The difficulties previously limiting the simultaneous computation of concentrations of many organic compounds were overcome by using a high-speed computer. The general method of White, Johnson, and Dantzig (*6*) was followed. By an iterative process, that distribution of species is found which minimizes the total free energy of the system while simultaneously satisfying the constraints on total elemental composition. At each stage $M + 1$ linear equations are solved, where M is the number of elements in the system.

The standard free energies of formation for the compounds were obtained from tables based on experimental results or by the method of group contributions suggested by van Krevelen and Chermin (*7*). In this latter method, advantage is taken of the fact that the free energy of an organic compound is nearly a sum of "group contributions" from its constituent bonds, branch points, rings, and symmetry numbers. Free-energy values for each group are derived from experimental values for a few compounds which contain it. The precision of the calculated free energies is within 2 kcal/mole for compounds similar to those measured and is usually much closer. The values for the major constituents CO_2, CH_4, H_2O, and CO are known much more precisely. If the free energy used for a minor compound is too high by 1 kcal, the concentration calculated will be too small by a factor of 0.36 at 500°K and 0.60 at 1000°K.

A detailed description of the method, tabulation, and documentation of free energy values and presentation and discussion of results is being prepared in monograph form (*8*).

In the general ternary diagram (Fig. 1) the main characteristics of ideal gas systems containing all proportions of the elements C, H, and O are shown. There are two pronounced thresholds at which concentrations of many compounds change abruptly by many orders of magnitude. The first is the oxidizing threshold along the CO_2–H_2O line, below which free O_2 appears and all organic compounds are oxidized; above this line traces of many organics appear in addition to CO_2, CO, H_2O, and CH_4. The second is the "asphalt" threshold above which large concentrations of benzene and polynuclear aromatics appear. The position of this line varies with temperature and pressure, in contrast to the oxidizing threshold which remains essentially unchanged. There is a weak hydrogen threshold along the CH_4–H_2O line which appears at low temperatures. For example, at 500°K and 1 atm, CO, CO_2, benzene, ethane, hexane, CS_2, COS, and so forth vary by several orders of magnitude in crossing this line. The curved line represents a phase boundary above which solid graphite would precipitate in a complete equilibrium.

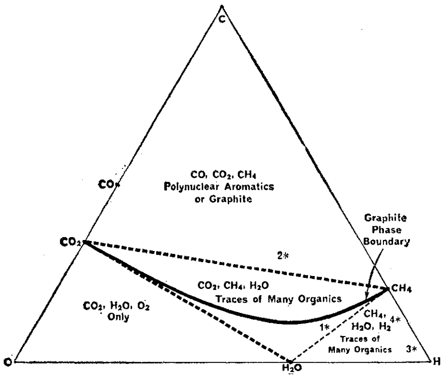

Fig. 1. Thermodynamic equilibria in atmospheres of varying elemental proportions. The ternary diagram provides a display of systems of all possible relative proportions of C, H, and O. The points corresponding to pure gases of the major compounds are indicated, and regions where different compounds are important are shown. The solid curve indicates the phase boundary along which graphite becomes stable at 1 atm and 500°K. The activation energy for this reaction is so high that under many conditions it does not occur and gaseous equilibria above this line are observed experimentally. Above the line CH_4—CO_2, equilibrium favors the formation of large proportions of polycyclic aromatic compounds and a lesser increase in most of the other families of compounds. The graphite and asphalt lines are always present, but their positions vary with temperature and pressure. The numbered asterisks indicate the compositions of the equilibrium distributions shown in Table 1.

The positions of the graphite phase boundary at various temperatures and pressures are shown in Fig. 2. In addition to the data illustrated, it may be noted that at 500°K and 10^{-6} atm and at 700°K at both 10^{-6} and 10^{-3} atm this line ends near the hydrogen corner.

Conventional equilibrium computations consider a very limited number of compounds, usually in single, reversible reactions. The balance of chemical species is computed for this extremely limited system as if no other reactions were occurring at the same time. Organic chemists know that this is frequently highly unrealistic; such a simplification is justified by necessity because more complex systems could not be considered in detail. With the use of high-speed digital computers, routine calculations of simultaneous reactions among a very large number of compounds is possible. In practical cases where time is important, complete equilibrium may be an unrealistic ideal. With rapid quenching, or at temperatures at which reactions require appreciable lengths of time to approach equilibrium, some reactions may occur only to a negligible extent. If the activation energy for all reactions leading to a particular product is high, and the temperature is sufficiently low, this product may be essentially "forbidden." All the other compounds of the system may have reached a metastable equilibrium after a certain time, while the particular compound is still present only in very small amounts.

As a way of simulating such conditions for purposes of computation, we use a method of limited equilibrium, in which all compounds of significant concentration are included except the few which are specifically excluded. In these calculations, the rate of production of each compound is assumed to be either rapid enough for equilibrium to be approximated, or negligible (zero). Experiments show that some reactions are indeed inhibited on a time scale of days at temperatures as high as 850°K (*5*). It should be noted that the actual production of small amounts of the forbidden compounds does not seriously disturb the proportions of the compounds in the quasi-equilibrium mixture. The method is a valid approximation as long as the forbidden compounds do not approach their final equilibrium concentrations.

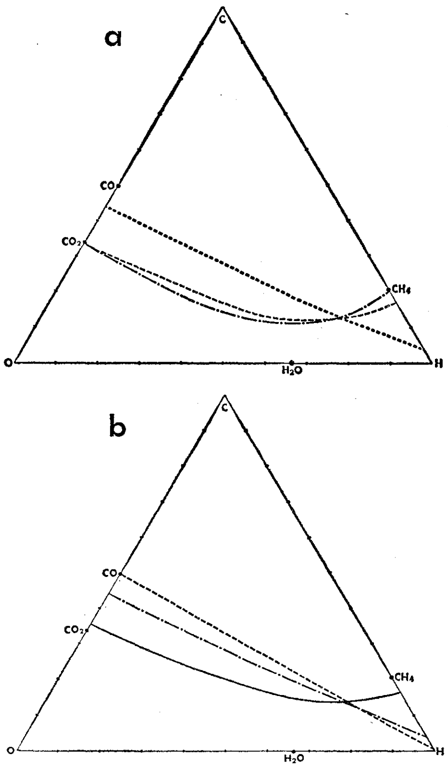

Fig. 2. Graphite phase boundaries. In an all-inclusive equilibrium, the gas phase would never have a composition above this phase boundary. However, the activation energy barrier to graphite formation is very high, so that under many conditions equilibrium may be approximated in metastable gases without any graphite formation. At 300°K a liquid water phase forms over the lower central portion of the figure. Outside this region, the graphite phase boundary is indistinguishable from the boundary at 500°K. (*a*) 1 atm; curves: dot-dash, 500°K; medium dashes (middle curve), 700°K; short dashes, 1000°K; (*b*) 1000°K; curves: solid, 50 atm; dot-dash, 1 atm; dashes, 10^{-3} or 10^{-6} atm.

According to a formally strict definition of thermodynamic equilibrium, graphite must be included as a major constituent of the system (*4*, *9*). However, at some temperatures there are reasons to exclude graphite from the computation and to use the method of limited equilibrium. Graphite is the end product of the polymerization of higher aromatic compounds, a relatively long sequence of reactions. At temperatures below about 850°K, it apparently cannot form directly from methane and other simple organics on a laboratory time scale, because the activation energy of such reactions would be too high. At lower temperatures as in petroleum deposits, the metastability persists on a geological time scale. At moderate temperatures, therefore, a metastable equilibrium of many other compounds could be approached before significant amounts of graphite could be produced. The elemental proportions represented by the region above the graphite line in the ternary diagram therefore give gas-phase compositions which can actually be attained experimentally. The exclusion of graphite permits these compositions to be studied, and the "asphalt region" to be investigated. If we had felt obliged to adhere to the strict definition of "equilibrium," many of these studies could not have been carried out. In some of the following computations, graphite has been excluded.

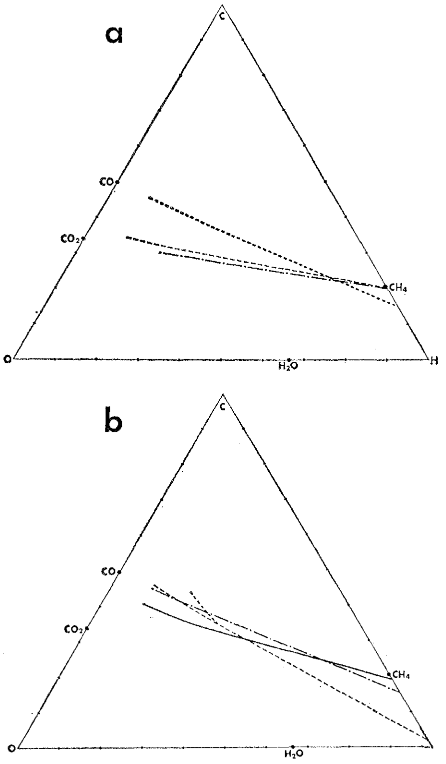

Fig. 3. Curves where benzene concentration is 10^{-6} mole fraction. (*a*) 1 atm; curves as in Fig. 2*a*. (*b*) 1000°K; curves: solid, 50 atm; dot-dash, 1 atm; medium dashes (almost straight line), 10^{-3} atm; short dashes, 10^{-6} atm. Benzene is found at 1000°K even in the presence of an excess of hydrogen. The curves for 10^{-3} atm and 10^{-6} atm at 1000°K are indistinguishable except for a slight divergence at the upper end. At 300°K the benzene concentration is slightly lower than 10^{-6} atm above the CO_2—CH_4 line and much lower elsewhere.

In Fig. 3 are shown boundaries above which the benzene concentration is greater than 10^{-6} mole fraction, an amount readily measured experimentally. At high temperatures and low pressures, benzene (and asphalt) appear even in an atmosphere containing a large excess of free hydrogen. This point is significant in theories concerning the formation of organic compounds in gas mixtures containing large excesses of hydrogen. Our result is consistent with the experimental findings of Studier *et al.* (*5*), who have proposed that such conditions may have existed in solar nebulas (*1*). The formation of asphalt in the presence of excess hydrogen is due to two mutually reinforcing factors. Firstly methane, a major constituent, becomes less stable with increasing temperature. Secondly, the equilibrium.

$$6\,CH_4 \rightleftharpoons 9\,H_2 + C_6H_6$$

shifts toward the right as the pressure decreases. Benzene and asphalt become measurable only in regions where solid graphite would be stable if it had been included in the equilibrium.

With graphite formation excluded, the concentrations of the other constituents change only gradually in the neighborhood of the graphite line; it is not a definite "threshold." Above the graphite line there are regions where the computed benzene concentration would become very high if benzene were the only aromatic included in the equilibrium. When higher molecular weight aromatics are included also, they become more important than benzene. The largest polynuclear aromatics often become so concentrated that they would precipitate. However, since the large molecules must build up from the small ones, the kinetics of a given situation dictate how far this polymerization will be able to go in the available time. We have approximated the condensation of polynuclear aromatics by including in our computation benzene, naphthalene, and a mixture we call "asphalt," which is a composite of 100 isomers having six benzene rings with the molecular formula $C_{22}H_{12}$. The free energy of this composite is computed by the method of group contributions (*7*). For each temperature and pressure the position of the asphalt threshold, where aromatics build up sharply, is insensitive to the exact formulas and free energies of the aromatics included in the equilibria. The threshold is sharper at lower temperatures and at higher pressures. Figure 4 shows lines above which the asphalt concentration is greater than 10^{-6} mole fraction for various conditions of temperature and pressure. Asphalt may form at all temperatures and pressures investigated. At high temperature and low pressure it is stable even in the hydrogen-rich region.

In the study of meteorites and geological deposits, the elements N, S, and Cl are also important. The addition of an amount of N equal to that of C produces very little change in the system. Molecular nitrogen remains prin-

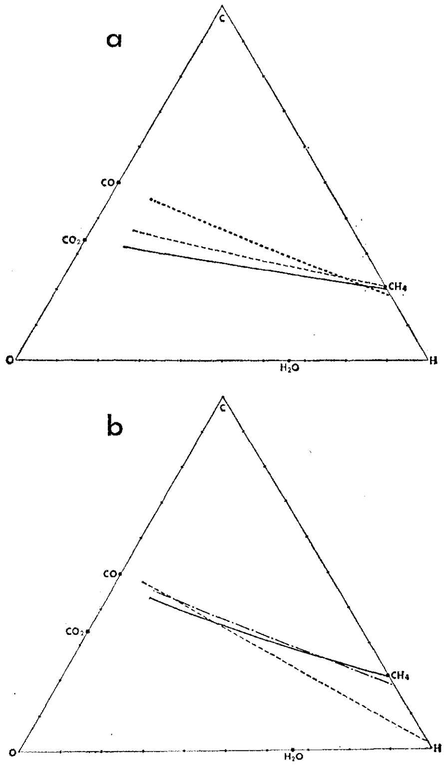

Fig. 4. Curves above which asphalt concentration is greater than 10^{-6} mole fraction. Graphite has been omitted from these systems for kinetic reasons. (*a*) 1 atm; curves: solid, 300° or 500°K; medium dashes (middle curve), 700°K; short dashes, 1000°K. (*b*) 1000°K; curves: solid, 50 atm; dot-dash, 1 atm; dashes, 10^{-3} or 10^{-6} atm. At 300°K the curves for pressures from 10^{-6} to 50 atm are very close together. Asphalt forms at all temperatures and pressures investigated. At high temperature and low pressure it is stable even where excess H_2 is present.

cipally as N_2, forming only traces of organics and oxides, a small amount of NH_3 in the presence of excess H_2, and a little HCN in the asphalt region. Formation of HCN is particularly favored by low pressure. NH_3 is favored by low temperature, high pressure, and high hydrogen concentration. In the atmosphere of Jupiter, it is the main nitrogen-containing compound. Rapid change of such a system might lead to products of a limited equilibrium in which N_2 did not participate. This would produce a relative increase in the concentrations of all other nitrogenous compounds.

Table 1 shows the mole fraction abundances of various compounds of interest at a temperature of 1000°K and pressures of 1 and 10^{-6} atm. The molar abundances of the new elements relative to carbon were $[N] = [C]$, $[S] = .0001 \times [C]$, and $[Cl] = .0001 \times [C]$. Mole fractions of constituents at the elemental composition points 1, 2, 3, and 4, shown in Fig. 1, are tabulated in Table 1. Point 1 is chosen below the graphite phase boundary and represents a strict, all-inclusive equilibrium. At the other three points, solid graphite formation was forbidden at 1000°K. It may be seen from the table that asphalt formation is encouraged by low pressure, so that it forms readily even in a system with a large excess of H_2. Low pressure also favors the decomposition of CH_4, CO_2, and NH_3.

In the asphalt region HCN and acetylene concentrations build up, as well as those of aromatics. Pyridine, the most stable of the nitrogen-containing aromatics is always less concentrated than benzene by several orders of magnitude.

The principal compound containing chlorine is HCl. Chloromethane, the most stable chlorinated hydrocarbon, is considerably less stable.

The most important sulfur compound is H_2S, except at low pressure in the asphalt region, where CS_2 is most important. Generally, organic sulfur compounds are much more stable than their oxygen analogs. This peculiarity may become important in theories of the origin of life. Carbon disulfide, methanethiol, benzenethiol, and thiophene

Table 1. Mole fraction compositions of compounds in equilibrium. The relative abundances of C, H, and O for the four points are shown in Fig. 1. N is as abundant as C. Cl and S are 0.0001 percent as abundant as C. Temperatures of 1000°K and pressures of 1 atm or 10^{-6} atm are considered. The four composition points have the following C:H:O ratios: point 1, 10:70:20; point 2, 30:50:20; point 3, 4:94:2; point 4, 12:86:2.

Elemental composition point (see Fig. 1)	1 Atm				10^{-6} Atm			
	1	2	3	4	1	2	3	4
H_2	0.54	0.11	0.86	0.55	0.55	0.37	0.91	0.81
O_2	$.59 \times 10^{-21}$	$.57 \times 10^{-26}$	$.15 \times 10^{-23}$	$.37 \times 10^{-25}$	$.52 \times 10^{-15}$	$.99 \times 10^{-35}$	$.25 \times 10^{-36}$	$.21 \times 10^{-36}$
H_2O	.15	$.92 \times 10^{-4}$	$.12 \times 10^{-1}$	$.12 \times 10^{-2}$	.15	$.14 \times 10^{-10}$	$.53 \times 10^{-11}$	$.43 \times 10^{-11}$
CO_2	$.55 \times 10^{-1}$	$.48 \times 10^{-3}$	$.56 \times 10^{-3}$	$.15 \times 10^{-3}$	$.53 \times 10^{-1}$	$.17 \times 10^{-10}$	$.32 \times 10^{-12}$	$.30 \times 10^{-12}$
CO	.14	.40	$.28 \times 10^{-1}$	$.48 \times 10^{-1}$	.15	.34	$.39 \times 10^{-1}$	$.41 \times 10^{-1}$
CH_4	$.55 \times 10^{-2}$	.19	$.55 \times 10^{-1}$	.25	$.63 \times 10^{-14}$	$.49 \times 10^{-4}$	$.21 \times 10^{-3}$	$.19 \times 10^{-3}$
C_2H_6	$.11 \times 10^{-7}$	$.68 \times 10^{-4}$	$.70 \times 10^{-6}$	$.22 \times 10^{-4}$	$.14 \times 10^{-31}$	$.13 \times 10^{-11}$	$.96 \times 10^{-11}$	$.89 \times 10^{-11}$
N_2	.10	.30	$.42 \times 10^{-1}$	.15	.10	.25	$.37 \times 10^{-1}$	.12
NH_3	$.69 \times 10^{-4}$	$.10 \times 10^{-4}$	$.89 \times 10^{-4}$	$.86 \times 10^{-4}$	$.70 \times 10^{-10}$	$.62 \times 10^{-10}$	$.91 \times 10^{-10}$	$.14 \times 10^{-9}$
HCN	$.41 \times 10^{-6}$	$.28 \times 10^{-3}$	$.13 \times 10^{-5}$	$.21 \times 10^{-4}$	$.45 \times 10^{-12}$	$.10 \times 10^{-1}$	$.43 \times 10^{-2}$	$.82 \times 10^{-2}$
Benzene	$.20 \times 10^{-18}$	$.76 \times 10^{-3}$	$.29 \times 10^{-14}$	$.12 \times 10^{-8}$	$<10^{-38}$	$.28 \times 10^{-5}$	$.53 \times 10^{-5}$	$.84 \times 10^{-5}$
Naphthalene	$.88 \times 10^{-30}$	$.41 \times 10^{-3}$	$.48 \times 10^{-23}$	$.18 \times 10^{-13}$	$<10^{-38}$	$.11 \times 10^{-5}$	$.13 \times 10^{-5}$	$.31 \times 10^{-5}$
"Asphalt"	$<10^{-38}$	$.33 \times 10^{-4}$	$<10^{-38}$	$.46 \times 10^{-29}$	$<10^{-38}$	$.68 \times 10^{-2}$	$.86 \times 10^{-3}$	$.80 \times 10^{-2}$
Formic acid	$.15 \times 10^{-7}$	$.26 \times 10^{-10}$	$.25 \times 10^{-9}$	$.42 \times 10^{-10}$	$.15 \times 10^{-13}$	$.33 \times 10^{-23}$	$.15 \times 10^{-24}$	$.13 \times 10^{-24}$
Acetic acid	$.24 \times 10^{-10}$	$.70 \times 10^{-11}$	$.24 \times 10^{-11}$	$.28 \times 10^{-11}$	$.26 \times 10^{-28}$	$.66 \times 10^{-28}$	$.52 \times 10^{-29}$	$.44 \times 10^{-29}$
Formaldehyde	$.10 \times 10^{-6}$	$.54 \times 10^{-7}$	$.32 \times 10^{-7}$	$.34 \times 10^{-7}$	$.10 \times 10^{-12}$	$.17 \times 10^{-12}$	$.47 \times 10^{-13}$	$.43 \times 10^{-13}$
Methanol	$.24 \times 10^{-8}$	$.25 \times 10^{-9}$	$.12 \times 10^{-8}$	$.85 \times 10^{-9}$	$.26 \times 10^{-20}$	$.28 \times 10^{-20}$	$.19 \times 10^{-20}$	$.16 \times 10^{-20}$
Ethanol	$.34 \times 10^{-13}$	$.63 \times 10^{-12}$	$.11 \times 10^{-12}$	$.52 \times 10^{-13}$	$.41 \times 10^{-37}$	$.50 \times 10^{-27}$	$.60 \times 10^{-27}$	$.50 \times 10^{-27}$
Ethylene	$.72 \times 10^{-8}$	$.22 \times 10^{-3}$	$.28 \times 10^{-6}$	$.14 \times 10^{-4}$	$.90 \times 10^{-26}$	$.12 \times 10^{-5}$	$.36 \times 10^{-5}$	$.38 \times 10^{-5}$
Acetylene	$.27 \times 10^{-10}$	$.42 \times 10^{-5}$	$.65 \times 10^{-9}$	$.49 \times 10^{-7}$	$.33 \times 10^{-22}$	$.64 \times 10^{-2}$	$.80 \times 10^{-2}$	$.93 \times 10^{-2}$
Xylene	$.16 \times 10^{-27}$	$.19 \times 10^{-7}$	$.88 \times 10^{-22}$	$.18 \times 10^{-14}$	$<10^{-38}$	$.37 \times 10^{-18}$	$.21 \times 10^{-17}$	$.35 \times 10^{-17}$
Acetone	$.97 \times 10^{-15}$	$.16 \times 10^{-10}$	$.12 \times 10^{-13}$	$.63 \times 10^{-12}$	$<10^{-38}$	$.27 \times 10^{-24}$	$.23 \times 10^{-24}$	$.22 \times 10^{-24}$
Dimethyl ether	$.81 \times 10^{-13}$	$.15 \times 10^{-11}$	$.26 \times 10^{-12}$	$.12 \times 10^{-11}$	$.97 \times 10^{-37}$	$.12 \times 10^{-26}$	$.14 \times 10^{-26}$	$.12 \times 10^{-26}$
Methylamine	$.23 \times 10^{-11}$	$.58 \times 10^{-10}$	$.18 \times 10^{-10}$	$.12 \times 10^{-9}$	$.26 \times 10^{-29}$	$.26 \times 10^{-19}$	$.67 \times 10^{-19}$	$.10 \times 10^{-18}$
Glycine	$.88 \times 10^{-20}$	$.20 \times 10^{-20}$	$.73 \times 10^{-21}$	$.13 \times 10^{-20}$	$<10^{-38}$	$<10^{-38}$	$<10^{-38}$	$<10^{-38}$
Pyridine	$.81 \times 10^{-22}$	$.14 \times 10^{-8}$	$.15 \times 10^{-18}$	$.14 \times 10^{-13}$	$<10^{-38}$	$.12 \times 10^{-12}$	$.77 \times 10^{-13}$	$.20 \times 10^{-12}$
S_2	$.74 \times 10^{-9}$	$.12 \times 10^{-6}$	$.50 \times 10^{-10}$	$.15 \times 10^{-8}$	$.32 \times 10^{-3}$	$.88 \times 10^{-7}$	$.18 \times 10^{-7}$	$.51 \times 10^{-7}$
CS_2	$.12 \times 10^{-8}$	$.17 \times 10^{-3}$	$.31 \times 10^{-9}$	$.98 \times 10^{-7}$	$.55 \times 10^{-9}$	$.26 \times 10^{-2}$	$.39 \times 10^{-3}$	$.12 \times 10^{-2}$
H_2S	$.20 \times 10^{-2}$	$.50 \times 10^{-2}$	$.84 \times 10^{-3}$	$.29 \times 10^{-2}$	$.14 \times 10^{-2}$	$.15 \times 10^{-4}$	$.17 \times 10^{-4}$	$.25 \times 10^{-4}$
SO_2	$.20 \times 10^{-10}$	$.25 \times 10^{-14}$	$.14 \times 10^{-13}$	$.18 \times 10^{-14}$	$.12 \times 10^{-4}$	$.37 \times 10^{-26}$	$.44 \times 10^{-28}$	$.59 \times 10^{-28}$
COS	$.17 \times 10^{-4}$	$.59 \times 10^{-3}$	$.87 \times 10^{-6}$	$.80 \times 10^{-5}$	$.11 \times 10^{-4}$	$.44 \times 10^{-6}$	$.23 \times 10^{-7}$	$.40 \times 10^{-7}$
Methanethiol	$.20 \times 10^{-8}$	$.86 \times 10^{-6}$	$.51 \times 10^{-8}$	$.13 \times 10^{-6}$	$.15 \times 10^{-20}$	$.19 \times 10^{-12}$	$.38 \times 10^{-12}$	$.57 \times 10^{-12}$
Benzenethiol	$.12 \times 10^{-23}$	$.56 \times 10^{-7}$	$.45 \times 10^{-20}$	$.10 \times 10^{-13}$	$<10^{-38}$	$.18 \times 10^{-12}$	$.16 \times 10^{-12}$	$.41 \times 10^{-12}$
Thiophene	$.20 \times 10^{-17}$	$.63 \times 10^{-6}$	$.32 \times 10^{-15}$	$.98 \times 10^{-11}$	$<10^{-38}$	$.13 \times 10^{-8}$	$.92 \times 10^{-9}$	$.21 \times 10^{-8}$
Cl_2	$.24 \times 10^{-15}$	$.11 \times 10^{-13}$	$.26 \times 10^{-16}$	$.50 \times 10^{-15}$	$.23 \times 10^{-15}$	$.23 \times 10^{-14}$	$.22 \times 10^{-16}$	$.24 \times 10^{-15}$
HCl	$.20 \times 10^{-2}$	$.59 \times 10^{-2}$	$.84 \times 10^{-3}$	$.29 \times 10^{-2}$	$.20 \times 10^{-2}$	$.51 \times 10^{-2}$	$.77 \times 10^{-3}$	$.24 \times 10^{-2}$
CH_3Cl	$.69 \times 10^{-9}$	$.36 \times 10^{-6}$	$.18 \times 10^{-8}$	$.44 \times 10^{-7}$	$.77 \times 10^{-21}$	$.23 \times 10^{-10}$	$.61 \times 10^{-11}$	$.19 \times 10^{-10}$
CCl_4	$.35 \times 10^{-33}$	$.62 \times 10^{-27}$	$.16 \times 10^{-34}$	$.63 \times 10^{-31}$	$<10^{-38}$	$.58 \times 10^{-33}$	$.38 \times 10^{-37}$	$.51 \times 10^{-35}$

are among the most stable sulfur-containing compounds.

The ethane-methane ratio is of interest, since this ratio was found to be 10^{-3} or less in some carbonaceous chondrites. It is smaller than that observed in fossil fuels or in photoactivated polymerizations or cracking processes (*1*). This ratio was computed to be less than 10^{-3} for all points illustrated in Table 1.

In the Fischer-Tropsch synthesis of hydrocarbons, the temperature can be kept low enough so that benzene does not form readily, presumably because the activation energies of all reactions leading to it are too high. In accordance with the method of limited equilibrium, we have therefore made computations in an otherwise all-inclusive system from which graphite, benzene, and all aromatic compounds are deleted. This leads to significant proportions of aliphatic compounds. A comparison of systems with and without aromatics is shown in Table 2. When aromatics are omitted, cyclopentane and cyclohexane are important. The larger aliphatic hydrocarbons are much more concentrated in this case than when benzene is present, the higher homolog mole fractions decreasing by a factor of ten for each additional carbon in the chain. Hydrocarbons with one double bond are slightly less stable than saturated ones. Those with a triple bond are considerably less stable. The ethane-to-methane ratio is .014. In the computed equilibrium, there is little difference in concentration between normal isomers and branched chains, in contrast to the preference for normal isomers experimentally observed in the Fischer-Tropsch synthesis. Of the oxygenated compounds, acetone, acetic acid, ketene, and acetaldehyde are most stable. Acetone is about as concentrated as octane. Traces of long-chain fatty acids are also predicted.

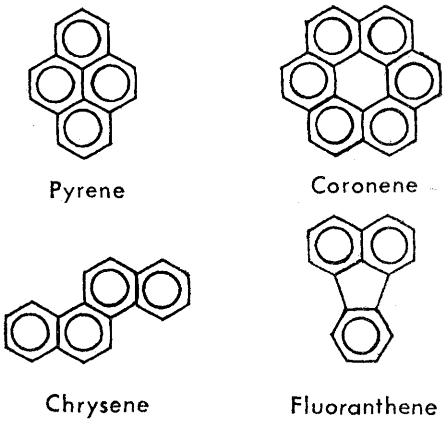

Fig. 5. Compounds detected in products of plasma discharge reactions.

When benzene and the other aromatics are included in this equilibrium, they are the most important organics. Higher homologs of all other families rapidly vanish. The ethane-to-methane ratio is 1.3×10^{-3}, and the concentrations of high homologs of the saturated hydrocarbons decrease by a factor of 300 for each increment in the number of carbon atoms. Here ethylene and acetylene are much less stable than ethane. These results are in qualitative agreement with the experimental results reported by Studier *et al.* (*5*), in which aliphatics, rather than aromatics, form when the temperature is kept sufficiently low. We take this as experimental support for the practical value of our method of limited equilibrium, in which, under appropriate conditions, selected products are excluded from a system otherwise at equilibrium. Because of the greatly varying rates of different reactions, this method of computation may be suitable in many cases. Those reactions whose rates are commensurate with the time available will approach equilibrium sufficiently closely for an order-of-magnitude determination of the proportions of the products. Other slower reactions will meanwhile have had only a negligible effect on the system. The validity of the computation, of course, depends on identifying the products which must be forbidden, as well as the major products which must be included.

Preliminary laboratory experiments which we have undertaken to test the above-mentioned theoretical conclusions have yielded the predicted results. By means of a radio-frequency oscillator and the auxiliary equipment described, in part, previously (*10*), it is possible to generate a plasma consisting of radicals, ions, and atoms from almost any compound having sufficient vapor pressure. When the energizing radio-frequency power is removed, such a plasma must tend toward a state of equilibrium, although the rapid rate of cooling may prevent its complete attainment. Compared to the time available during this cooling process, some reaction rates may be essentially zero, while others are relatively rapid. We believe that such conditions can be approximated by excluding from our computations certain compounds such as graphite,

Table 2. Mole fraction composition of gas mixture C:H:O = 30:40:30 at 1 atm pressure and 500° K. Graphite was omitted from the equilibrium in columns 2 and 5. Graphite and all aromatic compounds were omitted from the equilibrium in columns 3 and 6. Under these conditions, aliphatics are formed in high concentration.

Component	Aromatics included	Aromatics deleted	Component	Aromatics included	Aromatics deleted
H_2	0.94×10^{-4}	0.96×10^{-6}	Ketene	0.86×10^{-13}	0.50×10^{-9}
O_2	$<10^{-38}$	$<10^{-38}$	Formaldehyde	$.20 \times 10^{-11}$	$.14 \times 10^{-11}$
H_2O	$.11 \times 10^{-3}$	$.95 \times 10^{-8}$	Acetaldehyde	$.75 \times 10^{-11}$	$.44 \times 10^{-9}$
CO	$.41 \times 10^{-2}$	.29	Formic acid	$.13 \times 10^{-10}$	$.81 \times 10^{-13}$
CO_2	.61	.38	Acetic acid	$.20 \times 10^{-8}$	$.10 \times 10^{-8}$
Methane	.38	.32	Butyric acid	$.30 \times 10^{-14}$	$.10 \times 10^{-10}$
Ethane	$.66 \times 10^{-4}$	$.46 \times 10^{-2}$	Octanoic acid	$.14 \times 10^{-25}$	$.23 \times 10^{-14}$
Propane	$.80 \times 10^{-7}$	$.46 \times 10^{-3}$	Nonanoic acid	$.83 \times 10^{-29}$	$.11 \times 10^{-15}$
Butane	$.21 \times 10^{-9}$	$.99 \times 10^{-4}$	Palmitic acid	$<10^{-38}$	$.54 \times 10^{-2^{2}}$
Pentane	$.29 \times 10^{-12}$	$.11 \times 10^{-4}$	Methanol	$.21 \times 10^{-12}$	$.15 \times 10^{-14}$
Hexane	$.47 \times 10^{-15}$	$.15 \times 10^{-5}$	Ethanol	$.86 \times 10^{-14}$	$.52 \times 10^{-14}$
Heptane	$.73 \times 10^{-18}$	$.19 \times 10^{-6}$	Octanol	$.15 \times 10^{-31}$	$.29 \times 10^{-20}$
Octadecane	$<10^{-38}$	$.15 \times 10^{-16}$	Acetone	$.51 \times 10^{-11}$	$.25 \times 10^{-7}$
Cyclopropane	$.76 \times 10^{-13}$	$.42 \times 10^{-7}$	Dimethyl ether	$.51 \times 10^{-18}$	$.31 \times 10^{-18}$
Cyclobutane	$.23 \times 10^{-11}$	$.11 \times 10^{-3}$	Lactic acid	$.87 \times 10^{-22}$	$.33 \times 10^{-22}$
Cyclopentane	$.13 \times 10^{-11}$	$.48 \times 10^{-2}$	Oxalic acid	$.65 \times 10^{-13}$	$.26 \times 10^{-15}$
Cyclohexane	$.15 \times 10^{-13}$	$.46 \times 10^{-2}$	Pyruvic acid	$.71 \times 10^{-28}$	$.26 \times 10^{-26}$
Ethylene	$.88 \times 10^{-8}$	$.59 \times 10^{-4}$	Glycerol	$.71 \times 10^{-38}$	$<10^{-38}$
Propene	$.53 \times 10^{-9}$	$.29 \times 10^{-3}$	Carbon suboxide	$.24 \times 10^{-27}$	$.95 \times 10^{-20}$
Butene	$.92 \times 10^{-12}$	$.42 \times 10^{-4}$	Benzene	$.96 \times 10^{-4}$	
Octene	$.21 \times 10^{-23}$	$.43 \times 10^{-8}$	Naphthalene	$.73 \times 10^{-4}$	
Acetylene	$.55 \times 10^{-16}$	$.36 \times 10^{-10}$	Asphalt	$.11 \times 10^{-1}$	
Propyne	$.29 \times 10^{-16}$	$.16 \times 10^{-8}$	1,3-Butadiene	$.80 \times 10^{-14}$	$.36 \times 10^{-4}$
Octyne	$.15 \times 10^{-30}$	$.31 \times 10^{-13}$	Isoprene	$.26 \times 10^{-15}$	$.95 \times 10^{-4}$
Allene	$.35 \times 10^{-17}$	$.19 \times 10^{-9}$			

whose rate of formation is very slow. Since there are very abrupt changes in the concentrations of many compounds where the asphalt, hydrogen, and oxygen thresholds of the general C—H—O ternary diagram (Fig. 1) are crossed, it should be possible to map out experimentally the main features over the entire range of this diagram. The effects of other elements on the final composition of the systems may be similarly investigated.

Initial results with a simple carbon-hydrogen system indicate the presence of the asphalt barrier. Excitation of gases in which the ratio of hydrogen-to-carbon is less than four-to-one leads to the formation of tars consisting primarily of polynuclear aromatic compounds. Among these, pyrene, coronene, and chrysene (Fig. 5) have been identified so far; fluoranthene (Fig. 5) is also apparently present. Only minute traces of elemental carbon have been found. With water cooling we get practically all nonaromatic material, although products are at least partially unsaturated. In other words, the system appears to act as a limited equilibrium where aromatics are slow to form. This result is interesting in light of the computed results in Table 2, where aromatics have been excluded in a simulated limited equilibrium. If the hydrogen-to-carbon ratio is somewhat greater than four to one, the system appears in the hydrogen-rich region of the ternary diagram and only gaseous products are obtained. A detailed report of this work will appear at a later date. These experiments seem to demonstrate the plausibility of our use of the concept of "limited thermodynamic equilibrium."

R. V. Eck, E. R. Lippincott
M. O. Dayhoff, Y. T. Pratt
National Biomedical Research Foundation, 8600 16th Street, Silver Spring, Maryland, and
Department of Chemistry, University of Maryland, College Park

References and Notes

1. M. H. Studier, R. Hayatsu, E. Anders, *Science* **149**, 1455 (1965).
2. E. Anders, *Ann. N.Y. Acad. Sci.* **108**, 514 (1963); A. P. Vinogradov and G. P. Vdovykin, *Geokhimiya* **1964**, 843 (1964); W. G. Meinschein, *Space Sci. Rev.* **2**, 653 (1963); B. Nagy and D. J. Hennessy, *Ann. N.Y. Acad. Sci.* **108**, 553 (1963); N. H. Briggs and G. Mamikunian, *Space Sci. Rev.* **1**, 647 (1962–63).
3. M. O. Dayhoff, E. R. Lippincott, R. V. Eck, *Science* **146**, 1461 (1964). Professor Urey has kindly pointed out a slight error in the standard free energies used in these computations, a total of 0.38 kcal per mole for H_2, O_2, and N_2. This leads to a change by a small factor in calculated equilibrium concentrations for a few compounds. However, none of the conclusions are affected.
4. H. C. Urey and J. Lewis, *Science* **151**, 102 (1966); H. C. Urey, *ibid.*, p. 157.
5. M. H. Studier, R. Hayatsu, E. Anders, "Origin of organic matter in early solar system. I. Hydrocarbons," Enrico Fermi Inst. preprint 65-115 (1965). This work was also presented at the autumn meeting of the National Academy of Sciences, Seattle, Washington, 12 October 1965.

→ W. B. White, S. M. Johnson, G. B. Dantzig, *J. Chem. Phys.* **28**, 751 (1958).

7. D. W. van Krevelen and H. A. G. Chermin, *Chem. Eng. Sci.* **1**, 66 (1951); J. L. Franklin, *Mod. Eng. Chem.* **41**, 1070 (1949).
8. M. O. Dayhoff, E. R. Lippincott, R. V. Eck, G. Nagarajan, NASA report, in preparation.
9. H. E. Suess, *J. Geophys. Res.* **67**, 2029 (1962); S. L. Miller and H. C. Urey, *Science* **130**, 245 (1959).
10. F. X. Powell, O. Fletcher, E. R. Lippincott, *Rev. Sci. Inst.* **34**, 36 (1963); E. R. Lippincott, F. X. Powell, J. A. Creighton, D. G. Jones, in *Developments in Applied Spectroscopy*, vol. 3 (Plenum Press, New York, 1963).
11. Supported by NASA contract No. 21-003-002 with the National Biomedical Research Foundation, and NASA grant No. 21-002-059 to the University of Maryland.

7 March 1966

■

Mass-Yield Distribution of the Fission Products in Fallout from the 14 May 1965 Nuclear Explosion

Abstract. *Twenty single particles separated from a 20-liter sample of rain collected in Osaka, Japan, shortly after the 14 May 1965 test explosion of the Chinese nuclear device, were analyzed radiochemically. The abundance pattern of the fission products in these particles resembled the shape of the mass-yield curve for the thermal neutron-induced fission of uranium-235, except for the facts that cesium-h137 and strontium-90 were markedly depleted and the yields near the symmetric fission region appeared to be somewhat enhanced.*

The fallout of highly radioactive single particles occurs in Japan, because of the geographical location with respect to the nuclear weapons testing sites in the Asian mainland (*1*). Fission products appear to be highly fractionated in these particles, but there has been no attempt made in the past to investigate radiochemically the abundance patterns of the fission products in the particles.

A 20-liter sample of rain was collected on 20 May 1965 on the roof of the Radiation Research Center of Osaka Prefecture, Shinkecho, Sakai, Osaka, Japan (34°N, 135°E). The rain was evaporated to dryness and the residue was treated with a small quantity of distilled water. The slurry was spread over the surface of a filter paper (Whatman No. 40), dried, and then exposed to type KK Kodak x-ray film for 6 days. The autoradiograph thus obtained is shown on the cover of this issue.

The single particles thus located on the filter paper were punched out in circles 5 mm in diameter and further isolated by monitoring. The radius of these particles was estimated to be in the range of 5 to 15 μ. Twenty single particles were combined and were treated as follows.

Ten to 20 mg of Sr, Zr, Ru, Sb, Sn, Te, Cs, Ce, and La carriers were added to the sample and treated with HNO_3 and $HClO_4$, and the ruthenium was separated by distillation and further purified according to the method described by Rao (*2*). The residual material was treated with HNO_3, HF, and $HClO_4$, evaporated to a small volume, and treated with fuming nitric acid. The strontium fraction thus obtained was further purified radiochemically (*3*). The sulfides of Te, Sn, and Sb were precipitated from chloride medium, separated, and further purified (*4*). Zirconium and the rare earths were separated from Cs by hydroxide precipitation and the Cs was precipitated as $Cs_3Bi_2I_9$ (*5*). The Zr was separated from the rare earths and yttrium by anion exchange and further purified (*6*). The Ce was separated from Pm and Y by iodide precipitation (*6*) and the Pm and Y were separated from La by cation exchange (*7*).

The filter paper, from which the single particles were punched out, contained the bulk of the radionuclides

Table 1. Fission products in the combined sample of 20 single particles and in the bulk of rain concentrate collected in Osaka, Japan, on 20 May 1965.

Nuclide	Half-life (d, days; y, years)	Number *N* of atoms as of 14 May 1965 (10^6 *N*)	
		Single particles	Rain concentrate
Sr^{89}	50.4 d	N.D.*	2640 ± 500
Sr^{90}	28 y	89 ± 30	47200 ± 5000
Y^{91}	59 d	138 ± 45	4500 ± 1000
Zr^{95}	65 d	131 ± 30	3880 ± 400
Ru^{106}	1.0 y	8 ± 4	590 ± 100
Sn^{123}	125 d	N.D.*	160 ± 80
Sb^{125}	2.7 y	5 ± 3	750 ± 200
Te^{127m}	105 d	21 ± 10	600 ± 100
Cs^{137}	30 y	48 ± 25	37300 ± 4000
Ce^{144}	285 d	132 ± 25	2880 ± 400
Pm^{147}	2.7 y	23 ± 7	3700 ± 800

* N.D., not detected.